Journal of Visualization, Vol. 4, No. 4 (2001) 313-322

Pressure Sensitive Paint Evaluation on a Supercritical Wing at Cruise Speed

Mébarki, Y.*[1] and Le Sant, Y.*[2]

*1 National Research Council, Institute for Aerospace Research, Montreal Road, Ottawa, K1A0R6, Canada.
*2 Office National d'Etudes et de Recherches Aérospatiales, Département d'Aérodynamique Fondamentale et Expérimentale, 8 Rue des Vertugadins, 92190 Meudon, France.

Received 16 March 2001.
Revised 1 August 2001.

***Abstract*:** A comparative wind tunnel test of various Pressure Sensitive Paint (PSP) formulations has been performed at the Institute for Aerospace Research (IAR) 1.5 m × 1.5 m Trisonic Blowdown Wind Tunnel. The model under study is a prototype supercritical wing of a half model. The results are presented at the cruise Mach number: M = 0.74. The effect of the Reynolds number on the pressure distribution is assessed by varying the stagnation pressure of the flow. The evaluated paints all use the same porphyrin molecule as the luminescent sensor and the differences in sensitivity to pressure and temperature are a result of the PSP binder, which differs for each formulation. Examples of the processed results are given and the accuracy of the different PSP formulations is also discussed.

***Keywords*:** pressure sensitive paint, wind tunnel testing.

1. Introduction

Pressure Sensitive Paint (PSP) technique is an optical method allowing the measurement of the surface pressure distribution over a model. The phenomenon involved is based on the luminescence of organic compounds quenched by oxygen: when a light of appropriate energy excites these molecules, the emitted intensity is inversely proportional to the partial pressure of oxygen in the medium. These molecules are embedded in a permeable coating for practical application in aerodynamic testing. The emission intensity registered with a scientific CCD camera then depends on the air pressure at the film surface. Unlike conventional instrumentation (discrete pressure taps), the PSP technique provides a continuous pressure mapping. More details about the method can be found in Mosharov (1999), Coyle et al. (1999) and Bell et al. (2001).

The paper presents the consecutive evaluation of five different PSP formulations (using the usual intensity method) in the IAR 1.5 m × 1.5 m Trisonic Blowdown Wind Tunnel, on the same half-model at the cruise speed (M = 0.74) and for various Reynolds numbers. Although the wing is painted on both surfaces, the PSP measurements are performed only on the wing upper surface.

The interesting feature of the PSP formulations under consideration is that they use the same molecule as the oxygen sensor, thus enabling a unique excitation and reception setup for all the paints. However the binders that vary from paint to paint introduce differences in their sensitivities to pressure and temperature, response time or surface finish (Mébarki, 2000). Following a description of the model and the facility, the results obtained for some PSP formulations (M = 0.74) are presented. The paper concludes with an evaluation of the performance of the various PSPs at the nominal Mach number.

2. Materials

2.1 Wind Tunnel and Model

The high speed facility of the Institute for Aerospace Research (IAR) is a blowdown pressurized wind tunnel operating from low subsonic (M = 0.1) to supersonic (M = 4.5) regimes. For the present study, the tests have been conducted at M = 0.74 in the 1.5 m × 1.5 m transonic perforated wall test section. At this Mach number, the flow total pressure is varied from 1.4 bar to a maximum of 3.1 bar, which allows the unit Reynolds number to range from 18.7 mil/m to 49 mil/m.

The wing, made of steel, and the aluminum half fuselage were mounted on the external sidewall balance. The model, shown in Fig. 1, was originally a twelfth scale version of the Dash 8-100 aircraft. The new supercritical wing, tested without a nacelle, has a 0-degree sweepback measured at the 60% chord line. The x-axis, used in the following to measure the distances from the wing leading edge at a given wing section, is perpendicular to this 60% chord line (the y-axis in Fig. 1). The model overall length is 1.73 m, the wing span is 1.1 m and its mean aerodynamic chord is 0.2 m. The wing chord tapers from 0.3 m at the wing root on the fuselage to 0.1 m at the wing tip. In the following, for a given wing section located at a distance y from the model centerline, a point coordinate will be expressed by its distance from the wing leading edge (x) divided by the local chord ($c(y)$), or simply x/c.

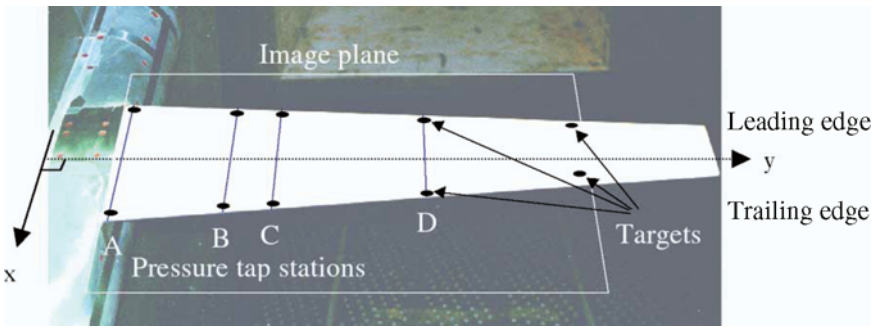

Fig. 1. Photograph of the half-model mounted in the test section: wing is coated with primer. Targets (not on scale) are used for image alignment and resection.

The airfoil sections, used to generate the wing, were designed by de Havilland and IAR to sustain extensive areas of laminar flow, when boundary layer transition was free. Therefore, to have the wing in its optimum configuration, the half-model is tested in this study with free transition. The wing is equipped with 4 rows of 32 pressure taps. These stations, designated as A, B, C and D, in Fig. 1, are respectively located at 11%, 27%, 35% and 57% of the wing span. Figure 1 also shows the targets used for PSP post-processing.

The coordinates of the selected targets must be known with good accuracy in the reference frame of the 3D-model. They are generally placed on the primer or directly on the PSP surface (case of Uni-Coat and FIB) by either means: Register Marks (Letraset 554, 7.5 mm diameter, 4 mm thick) or ink marks (4 mm-diameter using a fine point permanent marker). Removal of a disk of PSP active layer, appearing dark on the intensity images, can also play the same role.

For each PSP application, a new set of targets is applied. To avoid the measurements of the target physical coordinates (and the model removal) for each new PSP application, characteristic locations are preferred. Two pressure taps (x/c = 5% and x/c = 95%) on each row have been selected as well as a wing-flap junction and these physical coordinates have been measured prior to the test. Also shown in Fig. 1 is the image plane as viewed by the CCD camera using a lens focal length of 24 mm.

The ceiling of the test section is equipped with 20 optical windows. To provide a fairly uniform and stable illumination, 16 filtered (color filter KOPP 4-96) and cooled green halogen lamps are used (Iwasaki JY 1562 GR/N/CG 50 W). The digital CCD 1024 × 1024 Photometrics camera and an Infrared Agema 900 camera (136 × 272 pixels) are also mounted in the plenum shell. The CCD camera, equipped with 2 interference filters in parallel, Andover 650FS40 and Melles Griot 03FIB014, records the PSP emission from the wing root (station A) to approximately 85% of the wing span. The infrared camera focuses on three rows of taps (from station B to D),

thus covering 30% of the wing span. Although PSP measurements are only performed on the upper surface of the wing, the paint is applied on both upper and lower wing surfaces to evaluate its effect on the flow (Mébarki, 2000).

The duration of a run depends on the flow condition (Mach number and total pressure P_o). Table 1 summarizes the testing conditions selected for the cruise Mach number M = 0.74; the duration given in Table 1 is the maximum usable run duration (total run duration minus 2 seconds of flow establishment at startup). The given Reynolds number (R_c) is based on the mean aerodynamic chord.

Figure 2 illustrates the evolution of total pressure and temperature with time during a run for two flow conditions. The target total pressure is usually attained two seconds after the beginning of the run. For a given run, two parameters will limit the maximum number of images: the exposure time, depending on the PSP and the pressure level, and the digitization rates of the CCD camera (500 kHz).

During the 2 second delay needed for image digitization and storage, the model is pitched to its next target angle of attack (at a maximum pitching rate of 10°per second) and is paused there, waiting nearly 2 seconds for the end of digitization. The conventional pressure and force measurements are then synchronized with the image acquisition. This type of acquisition is called pitch-pause in contrast with a continuous pitch mode, not compatible with the present PSP time response.

Table 1. Testing conditions

M	R_c ($\times 10^6$)	P_o (bar)	α (°)	Duration (s)
0.74	3.81	1.41	0, 1, 3, 5	37
	5.54	2.04	0, 1, 3, 5	21
	8.51	3.14	1, 3, 5	11

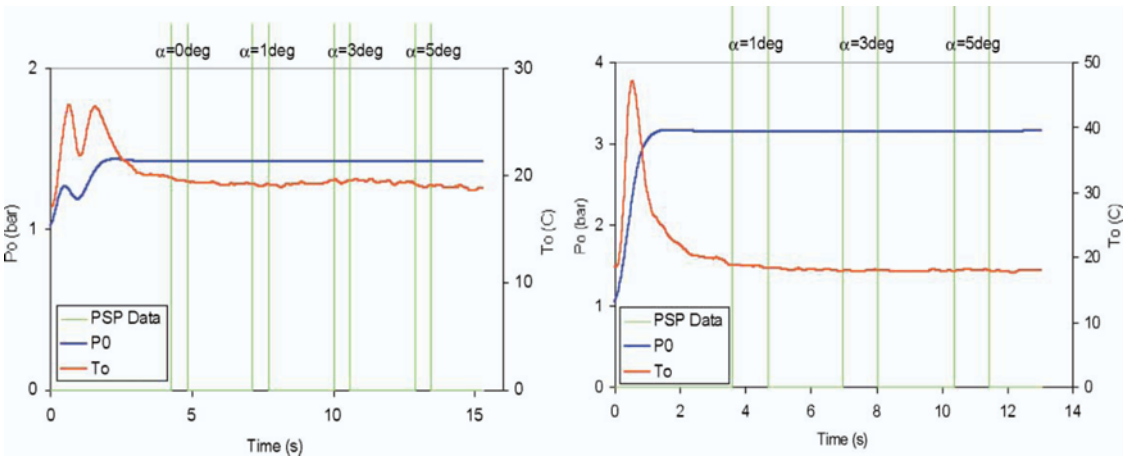

Fig. 2. Example of PSP acquisition during a run; left: M = 0.74, R_c = 3.8 x10^6, right: M = 0.74, R_c = 8.5x10^6.

Large temperature variations may follow the tunnel startup and the PSP measurements are delayed until the total temperature has recovered to ambient levels, while the model is being set to the first angle of attack (e.g. $\alpha = 0°$ or 1°). Also, between the first and the last PSP images, the total temperature decreases slowly by 0.5°C at low R_c and 1°C at high R_c. The reference images (one for each angle of attack) are recorded before the run at ambient temperature. This reference (wind off) temperature, given by a thermocouple placed on the wing, is usually close to the initial T_o, or T_o (t = 0) in Fig. 2, and a global temperature variation between reference and run measurements is to be expected.

2.2 Pressure Sensitive Paint

All PSP formulations under study use the same porphyrin molecule (PtFPP) as the oxygen sensor. Therefore, the optical system described above (green halogen lamp, excitation and reception filters) is suitable for all the PSP formulations. Two formulations, one from IAR (noted as PSP PAR), and the PSP FEM developed by Oglesby and Upchurch (1999), from NASA LaRC, are not commercially available. Three additional paints were supplied by Innovative Scientific Solutions Inc. (ISSI).

Table 2. PtFPP-based PSP under study.

PSP	Primer	Ref.	Source
FIB	Epoxy Tristar	(Gouterman and Carlson, 1999)	ISSI
Sol-gel	ISSI primer	(Jordan et al, 1999)	ISSI
Unicoat	no primer	(Mébarki, 2000)	ISSI
FEM	Epoxy Tristar	(Oglesby and Upchurch, 1999)	NASA LaRC
PAR	Epoxy Tristar	(Mébarki, 2000)	IAR

FIB PSP, initially developed at the University of Washington, as well as the sol-gel PSP and the Uni-Coat PSP are produced commercially by ISSI. Table 2 gives the name and the origin of each PSP. Except in the case of the Uni-Coat formulation, which does not require a primer coating, the commercial FIB and sol-gel formulations are supplied with their respective primer.

To simplify the application procedure as well as to solve adhesion problems, the FIB active layer is applied on top of a white epoxy primer (Tristar DHMS C4.01TY3). This primer is also used as the primer layer for both the FEM and the PAR. The binder or permeable matrix in which this porphyrin molecule is dissolved will cause different pressure and temperature sensitivities. Usually the primer has no effect on the pressure or the temperature sensitivity of the pressure sensitive coating applied on top. Because an effect of the support (bare metal or primers) on the PSP response has already been reported in the case of the FIB (Puklin, 1998), the effect of the epoxy primer on the FIB response was investigated prior to the test. No modification of the FIB performance was observed on the prepared samples.

To compare the various PSP performance, the effect of temperature on the pressure sensitivity $SP = D(I_{ref}/I) / DP$ (slope of the Sten-Volmer plot in % per bar) and the evolution of the temperature sensitivity $ST = - D(I/I_{ref})/DT$ (in % per degree) with the pressure are considered. The pressure sensitivity was calculated between 0.15 bar and 2 bar and the temperature sensitivity was determined between 10°C and 35°C on samples prior to the wind tunnel investigation.

The various PSP formulations present a temperature sensitivity (note the opposite sign in the expression of *ST* given above) between 0.6% to 1.6% per degree. This sensitivity is affected by the pressure level for all the formulations except in the case of the FIB (see Fig. 3 right). The pressure sensitivity, also dependent on the binder used, varies from 55 to nearly 80% per bar and is diversely affected by the temperature. In particular, the same pressure sensitivity *SP* (60% per bar at 20°C) and a similar linear dependence on temperature can be observed in the case of Uni-Coat and sol-gel formulations (see Fig. 3 left). A summary of the PSP characteristics is given in Tables 3 and 4. The given thickness concerns only the PSP sensitive coatings; it excludes the primer thickness (roughly 25 mm).

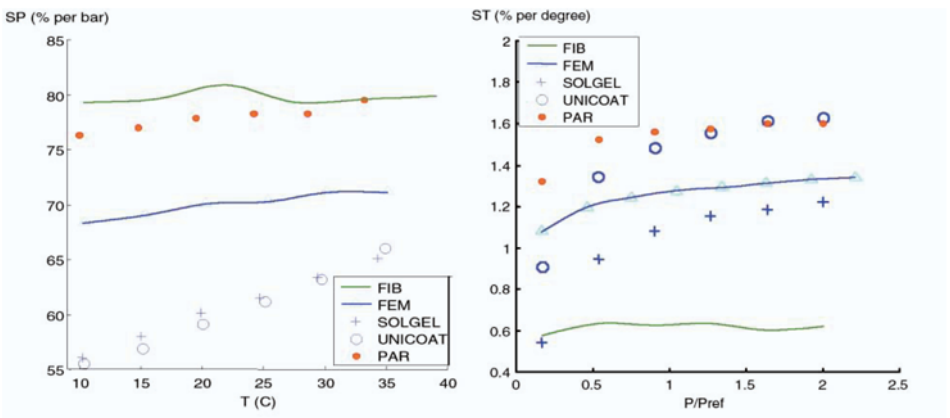

Fig. 3. Evolution of the PSP sensitivity to pressure (left) and to temperature (right) (see text for definition) with pressure: P_{ref} = 1 bar, T_{ref} = 10°C.

Table 3. Pressure sensitivity (*SP*) and temperature sensitivity (*ST*) of PSP tested.

PSP	Pressure Sensibility (% per bar @ 20°C)	Temperature Sensibility (% per °C @ 1 bar)
FIB	80.57	0.63
Sol-gel	60.23	1.09
Uni-Coat	59.04	1.51
FEM	70.01	1.27
PAR	77.85	1.57

Table 4. Characteristics of the Pressure Sensitive Paints tested on the half-model. The surface finish, using non-contact Vertical Scanning Interferometry (WYKO-NT2000 system), and the time response were estimated on samples painted separately from the model.

PSP	Thickness (mm)	Targets with respect to PSP active layer	Surface finish *Ra* (mm)	Time Response (s)
FIB	8	Over	0.9	0.75
Sol-gel	8	Underneath	NA	NA
Uni-Coat	20	Over	0.6	25
FEM	5	Underneath	0.17	0.85
PAR	4	Underneath	0.15	1

The implementation of the PSP technique in a pressurized and blowdown facility requires paints with a reasonably fast response time (equal or lower than the flow establishment duration).

The IAR PSP laboratory has not been designed for unsteady analysis. However, for a thickness of the active layer below 10 mm, the response time of the coatings is estimated to be lower than the flow establishment duration occurring at startup (roughly 2 seconds). Consequently, the PSP active layers were applied on the model with an average thickness of 4 mm (FEM, PAR) and 8 mm (FIB, sol-gel). A thin and uniform application of the Uni-Coat was difficult to obtain because it is the only PSP active layer that comes in a spray-can and fine airbrush adjustments are not available. In the case of the thick layer of Uni-Coat on the wing (e = 20 mm in average), the response time, estimated to be nearly 25 seconds, exceeds the duration of most of the runs (see Table 1).

Having a model equipped with pressure taps, discrete measurements are available to convert intensity ratio to pressure: this simple method is called *in situ* calibration. It consists in computing the optimum (in the least square sense) third-order polynomial interpolation between the intensity ratio extracted nearby the tap locations and the discrete pressure data of the corresponding run. The calibration coefficients and the resulting rms error are calculated using a total of 39 taps on all stations B, C and D satisfying the condition ($0.05 < x/c < 0.95$): the station A located inboard, not totally visible for high angles of attack, is excluded.

3. Results

The image registration is performed using AFIX2 software developed at ONERA (Le Sant et al., 1997). The image conversion from the measured intensity into pressure coefficient (or Cp) is performed in Matlab, using in-house routines. Since the complete data reduction is automated, it requires less than 2 minutes per processed image.

The comparison between PSP results, using the *in situ* calibration, and the pressure taps is shown in Fig. 4 on two stations for all incidences at $M = 0.74$, $R_c = 3.8 \times 10^6$. In this example, the average error on all images, all stations (B, C and D), is 0.02 in Cp or 1.4% of the full pressure scale measured on the 39 taps used for the PSP calibration.

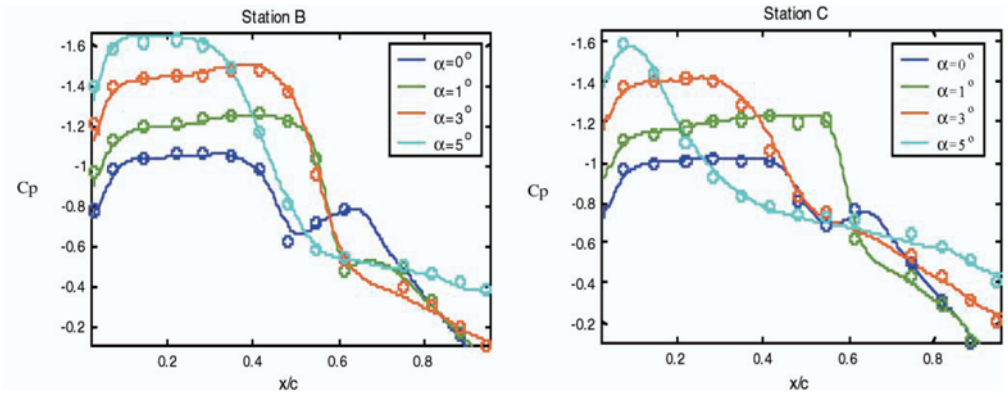

Fig. 4. Comparison of PSP results with pressure taps for FIB PSP at $M = 0.74$ using *in situ* calibration.

As shown in Fig. 5, the shock location on the wing upper surface is much closer to the leading edge at station C than it is at station B for the highest incidence ($a = 5^\circ$). This is not an effect of the PSP coating on the flow, since it was also measured on the bare metal (PSP OFF) wing, at the same station C and for the same flow condition. The Cp images obtained from FIB PSP measurements for this condition are presented in Fig. 5. The local shock displacement around station C is already visible at $a = 3^\circ$ and extends further at $a = 5^\circ$.

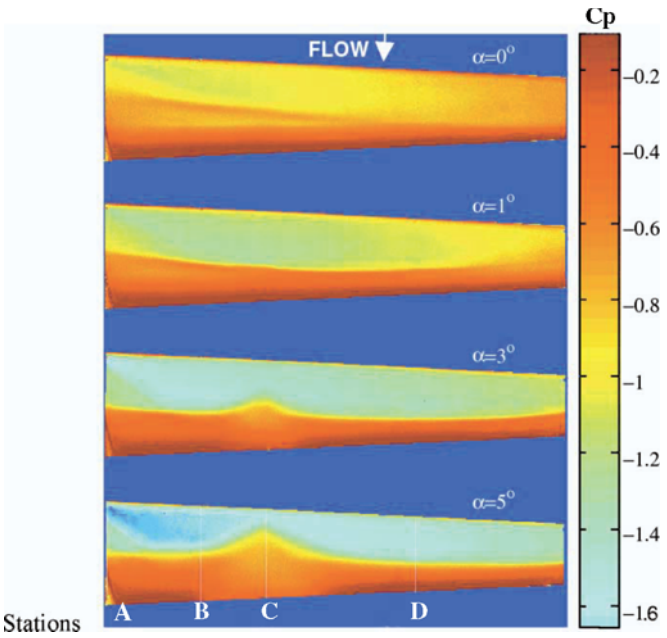

Fig. 5. PSP results obtained with FIB PSP at $M = 0.74$, $R_c = 3.8 \times 10^6$ at various angles of attack. $Cp_{cr} = -0.62$.

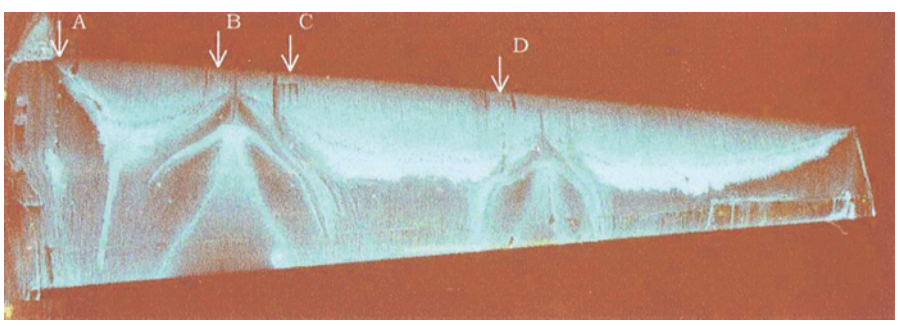

Fig. 6. Fluorescent oil flow visualization at $M = 0.74$, $R_c = 3.8 \times 10^6$ and $a = 5^\circ$. Direction of flow is from top to bottom. Tap stations indicated.

Following this observation, fluorescent oil flow visualization on the bare metal wing have revealed the presence of a separated flow region with reverse flow occurring at $M = 0.74$, $R_c = 3.8 \times 10^6$, $a = 5^\circ$. Additional visualizations at this flow condition have shown that the origin of the flow separation is likely to change, from station C to station B (located inboard). In some cases, a similar and smaller separated flow region was observed outboard of station D (around 70 % of the wing span).

Figure 6 shows an example of oil flow visualization on the bare metal wing, obtained at the same flow condition (M= 0.74, $R_c = 3.8 \times 10^6$, $a = 5^\circ$), when two separated flow regions were present on the wing upper surface. The inboard flow separation coincides exactly with the right edge of a leading edge insert (station B this time), whereas the flow separation outboard seems to be initiated by local dust contamination.

It is interesting to note that a similar flow pattern has already been reported by Kawamoto et al. (1990) for a 2-D supercritical BGK1 airfoil tested in the NAL 2-D wind tunnel (Fig. 7). Sudani et al. (1990) have also shown that the lateral suction of the sidewall boundary layer influences the dimension of the flow separation occurring on the upper surface of the supercritical airfoil.

In our study, the PSP measurements, providing a complete and detailed pressure distribution, have immediately revealed an unexpected pressure field at high incidence, difficult to pinpoint with only few stations of pressure taps on the wing. It must be noted however that the flow separation (shown in Figs. 5 and 6) occurred on the wing upper surface for a Reynolds number lower than that usually tested with this model ($R_c = 8 \times 10^6$).

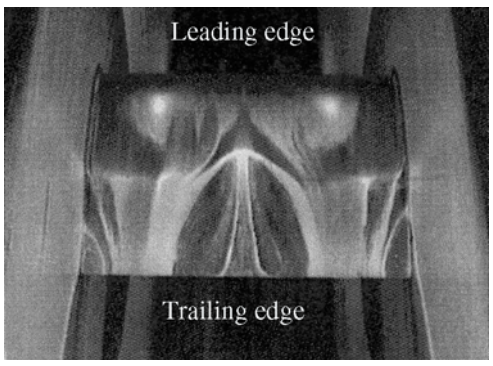

Fig. 7. Fluorescent oil flow visualization at $M = 0.75$, $R_c = 6.5 \times 10^6$ and $a = 5^\circ$ on the upper surface of 2-D BGK1 supercritical airfoil performed at the 2-D NAL wind tunnel in Japan. Flow is from top to bottom. No lateral boundary layer suction applied. Reproduced from Kawamoto et al.(1990) with permission.

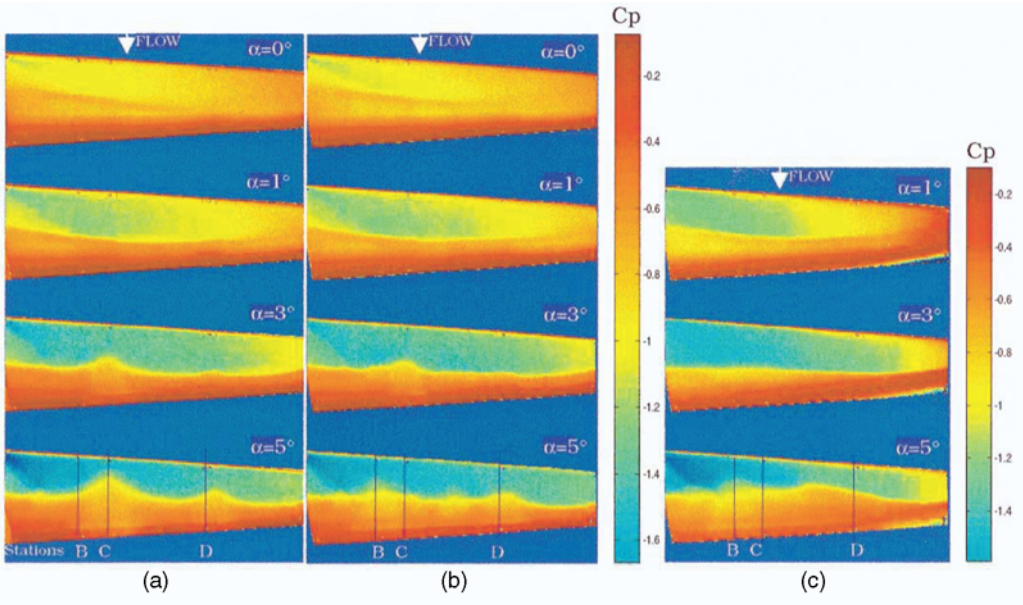

Fig. 8. Effect of the Reynolds number on the wing upper surface. Cp distribution measured with PSP Uni-Coat for (a) $R_c = 3.8 \times 10^6$, (b) $R_c = 5 \times 10^6$ and (c) $R_c = 8.5 \times 10^6$, *In situ* calibration.

The effect of the Reynolds number on the pressure distribution at $M = 0.74$ is presented in Fig. 8. The Cp scale is automatically determined using the minimum and the maximum values for each run. As a result, the pressure coefficients obtained at low ($R_c = 3.8 \times 10^6$) and moderate ($R_c = 5 \times 10^6$) Reynolds numbers are presented in Fig. 8 using the same scale, slightly different from that of the high Reynolds number configuration ($R_c = 8.5 \times 10^6$).

The Uni-Coat time response greatly exceeds the run duration at high Reynolds number, therefore these results are presented only for a qualitative assessment of the Reynolds number effect. The shock shape and location on the upper surface of the wing looks very similar at low angle of attack ($a = 1^\circ$) for the three Reynolds numbers, whereas the sharp shock curvatures noted at low Reynolds number and for the highest angle of attack disappear gradually with increasing Reynolds number. This observation was confirmed with paints such as the FIB, the FEM or the PAR, with shorter time response.

It has been also noted that the FEM or the PAR coatings, although smoother and thinner than the Uni-Coat, induced larger modifications of the wing aerodynamic performance for high Reynolds number. At angles of attack above $a = 2.5^\circ$, the lift measured with the smoother coatings was reduced compared to that obtained with the Uni-Coat formulation on the wing (Mébarki, 2000). These balance measurements were confirmed by the PSP results shown in Fig. 9. At $a = 5^\circ$ the shock location, limiting the supersonic flow region on the wing top surface, is closer to the wing leading edge inboard of station C than it is with the Uni-Coat on the wing (e.g. notice the wing-fuselage interaction still present on the Fig. 8 (c) at $a = 5^\circ$).

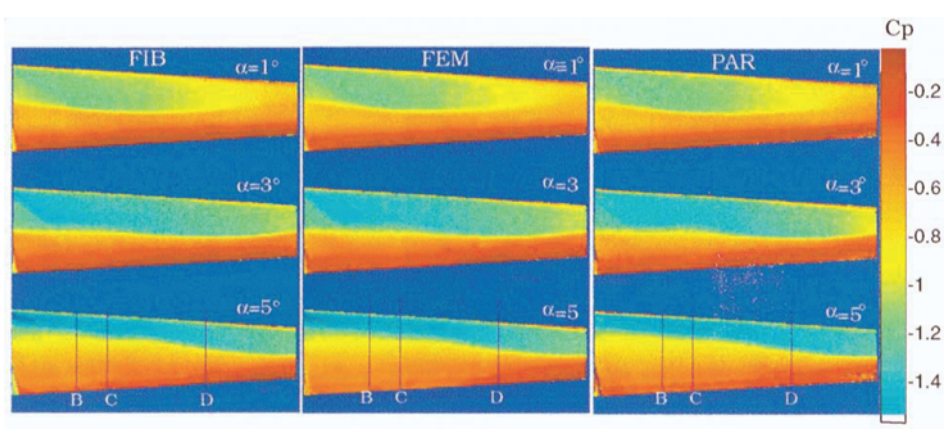

Fig. 9. Cp distribution on the wing upper surface at $M = 0.74$, $R_c = 8.5 \times 10^6$ for the PSPs FIB, FEM and PAR, *in situ* calibration. Flow direction is from top to bottom. Stations B, C and D indicated.

4. Accuracy

The accuracy of the PSP results, summarized in table 5, is computed from the quadratic difference between discrete and PSP measurements at the same location. This difference is expressed in terms of absolute Cp and percentage of the full-scale (*%fs*). The full-scale is the maximum Cp range measured during a run on the wing upper surface by the 39 taps used for the PSP calibration.

At the lowest Reynolds number, the accuracy is relatively good for all paints, despite their difference in temperature sensitivity. The infrared measurements have shown that the spanwise temperature gradient (between station B and D) measured for the FEM runs was low (below 1°C), whereas it was slightly above 2°C in the test performed with the FIB. The small temperature gradient along the chord (below 2°C in most cases) measured with the infrared camera, also explains the good performance obtained at low Reynolds number.

Also included in Table 5, is the exposure time used for all PSP formulations. The wind-on exposure time is set to avoid saturation at the minimum pressure, which is atmospheric pressure in the case of high Reynolds number. At this Reynolds number, the intensity measured at atmospheric pressure (during wind-off) is nearly the same for all PSPs (roughly 3500 counts measured by the 12-bit camera).

The exposure time t (in ms) is listed in Table 5 to illustrate the difference between formulations. For a given excitation, the emission intensity depends on the absorption coefficient of the sensor (the same in all cases), the concentration of the luminescent molecule and the active layer thickness. The Uni-Coat thickness ($e = 20$ mm), only two to four times larger than the other PSP active layers, allows very short exposure times.

Table 5. Absolute and relative errors in Cp and in % of the full scale of PSP formulations at $M = 0.74$. Dynamic pressure $q = 0.82$ bar and $q = 0.37$ bar for lowest and highest Reynolds number respectively.

PSP	$R_c = 3.8 \times 10^6$			$R_c = 5.4 \times 10^6$			$R_c = 8.5 \times 10^6$		
	t (ms)	DCp	*%fs*	t (ms)	DCp	*%fs*	t (ms)	DCp	*%fs*
FIB	500	0.02	1.4	–	–	–	1000	0.03	2.7
Sol-gel	125	0.04	2.8	–	–	–	250	0.04	3.1
Uni-Coat	50	0.04	3.2	50	0.04	3.7	75	0.10	8.4
FEM	500	0.02	1.7	–	–	–	1000	0.04	3.3
PAR	250	0.03	2.2	–	–	–	500	0.03	2.6

However, as a result of its thickness and slow response time, the PSP Uni-Coat cannot follow the pressure step (static pressure $P_i = 2.2$ bar, dynamic pressure $q = 0.83$ bar) at the highest Reynolds number, in the short time required (11 seconds). Meanwhile, it remains temperature sensitive and a spanwise temperature gradient still influences the accuracy of the pressure measurements. For example, a temperature variation of 1.5°C at the highest Reynolds number leads to a difference in Cp of 0.057 (or 46 mbar) for the Uni-Coat formulation. On the other hand for the same Reynolds number, a temperature difference of 1.2°C leads to a Cp variation of 0.02 in the case of the FIB formulation.

Additional sources of error may be due to resection errors induced by local discrepancies between the 3-D grid and the physical model (1 pixel on average as observed on the 8 pressure taps chosen as targets). In addition, errors in the image alignment (between wind off and wind on) are related to the wing deformation under the flow, especially near the wing tip. This is not taken into account by AFIX2 software, although the final accuracy of the alignment is on average lower than 1 pixel (or 0.075 cm) on the targets used for resection. The impact of these local errors on the global accuracy has not been assessed. Nevertheless, these error sources apply to all the PSP formulations in the same way and it should not affect the comparative evaluation.

5. Conclusion

The evaluation of five different pressure sensitive paint formulations in the IAR 1.5 meter blowdown wind tunnel is presented. The model under study is a supercritical wing of a half model, tested at a nominal Mach number $M = 0.74$.

The PSP technique has revealed a complex flow separation at the lowest Reynolds number, confirmed using oil flow visualization. The comparison of the various PSP performance at different Reynolds has been presented in terms of absolute and relative difference between the PSP results and the discrete measurements given by the pressure taps at three stations.

Acknowledgments

The authors wish to express their gratitude to Don Oglesby and Jeffrey Jordan, from NASA LaRC, for kindly providing the FEM formulation and reviewing the content of this paper. Thanks to Xin Lu and Prof. Mitchell A. Winnick from the Department of Chemistry of University of Toronto for collecting and providing the surface roughness data. Special thanks are due to Michel Grenier and Jim Thain from the IAR High Speed Wind Tunnel Groups and to Richard Poole, formerly of de Havilland (Toronto), for their contribution and assistance during the test.

References

Bell, J. H., Schairer, E. T., Hand, L. A. and Mehta, R. D., Surface Pressure Measurements Using Luminescent Coatings, Annu. Rev. Fluid Mech., 33 (2001), 155-206.

Coyle, L. M., Chapman, D., Khalil, G., Schibli, E. and Gouterman, M., Non-monotonic Temperature Dependence in Molecular-referenced Sensitive Paint (MR-PSP), Journal of Luminescence, 82-1 (1999), 33-39.

Gouterman, M. and Carlson, W. B., Acrylic and Fluorocacrylic Polymers for Oxygen Sensing and Pressure-sensitive-paints Utilizing These Polymers, US Patent N. US5965642 (1999).

Jordan, D. J., Watkins, N., Davis, P. N., Weaver, W. L., Dale, G. A., Navarra, K. R., Urban, J. R., Devoid, E. and Strange, R. A., Pressure Sensitive Paint Measurement in the Large-scale Commercial Engine-test Stand, ICIASF Conference Proceedings (Toulouse), (1999).

Kawamoto, I., Miwa, H., Baba, S., Sato, M., Kanda, H. and Sudani, N., Recent Airfoil Tests in NAL 2D High Reynolds Number Wind Tunnel, Proceedings of the 28th Aircraft Symposium (in Japanese), (1990).

Le Sant, Y., Deleglise, B. and Mébarki, Y., An Automatic Image Alignment Method Applied to Pressure Sensitive Paint Measurements, ICIASF Conference, (1997).

Mébarki, Y., Pressure Sensitive Paints: From Laboratory to Wind Tunnel, Proceedings of the ICAS 2000 Conference, (Harrogate, UK), (2000).

Mosharov, V. E., Binary Pressure Sensitive Paint: A Lot of Problems, 7th Annual Pressure Sensitive Paint Workshop, Purdue University, (1999).

Oglesby, D. and Upchurch, B., In Pursuit of the Ideal Pressure Sensitive Paint, 7th Annual Pressure Sensitive Paint Workshop, Purdue University, (1999).

Puklin, E. Ideal Pressure Sensitive Paint: PfTFPP in FIB polymer, 6th PSP Workshop (Seattle, Washington), (1998).

Sudani, N., Sato, M., Kanda, H. and Matsuno, K., Flow Visualization Studies on Sidewall Effects in Two-dimensional Transonic Airfoil Testing, AIAA paper No. 93-0090, (1990).

Author Profile

Youssef Mébarki: He obtained his Ph.D. from the University of Lille, France, in the field of Mechanical Engineering under the supervision of Pr. Stanislas (Ecole Centrale de Lille). His Ph.D. thesis was about the development and the application of the Pressure Sensitive Paint technique for aerodynamic testing at ONERA (Office National d'Etudes et de Recherches Aérospatiales) Meudon (France) in the Wind Tunnel Instrumentation and Optical Metrology group headed by Yves Le Sant. He joined the Institute for Aerospace Research of the National Research Council (NRC), Canada, in 1998 where he is presently a Research Officer. His current research activities include implementation of Pressure Sensitive Paint technique, analysis of the PSP intrusiveness and development of original paint formulations for NRC wind tunnels.

Yves Le Sant: He graduated from the Ecole Nationale Supérieure des Arts et Métiers (ENSAM) in 1982. He joined ONERA (Office National d'Etudes et de Recherches Aerospatiales) in 1983 to develop an adaptive wall test section for low supersonic tests. Then he developed a wall correction method for 3D transonic tests. His current work is to develop optical methods as heat flux assessment using infrared thermogaphy, Temperature Sensitive Paint and Pressure Sensitive Paint.